

Guggino, G. et al. (2021) Inflammasome activation in Ankylosing Spondylitis is associated to gut dysbiosis. *Arthritis and Rheumatology*, 73(7), pp. 1189-1199

The material cannot be used for any other purpose without further permission of the publisher and is for private use only.

There may be differences between this version and the published version. You are advised to consult the publisher's version if you wish to cite from it.

This is the peer reviewed version of the following article:

Guggino, G. et al. (2021) Inflammasome activation in Ankylosing Spondylitis is associated to gut dysbiosis. *Arthritis and Rheumatology*, 73(7), pp. 1189-1199, which has been published in final form at: [10.1002/art.41644](https://doi.org/10.1002/art.41644)

This article may be used for non-commercial purposes in accordance with [Wiley Terms and Conditions for Self-Archiving](#).

<http://eprints.gla.ac.uk/232608/>

Deposited on 03 February 2021

DR. GIULIANA GUGGINO (Orcid ID : 0000-0003-2479-6958)

PROF. DIRK ELEWAUT (Orcid ID : 0000-0002-7468-974X)

PROFESSOR RANJENY THOMAS (Orcid ID : 0000-0002-0518-8386)

PROF. FRANCESCO CICCIA (Orcid ID : 0000-0002-9352-1264)

Article type : Full Length

Inflammasome activation in Ankylosing Spondylitis is associated to gut dysbiosis

Giuliana Guggino MD, PhD^{1*}, Daniele Mauro MD, PhD^{2*}, Aroldo Rizzo MD³, Riccardo Alessandro PhD⁴, Stefania Raimondo PhD⁴, Anne-Sophie Bergot PhD⁵, M Arifur Rahman PhD⁵, Jonathan J. Ellis PhD⁶, Simon Milling PhD⁷, Rik Lories MD PhD⁸, Dirk Elewaut MD PhD⁹, Matthew A. Brown MD PhD⁶, Ranjeny Thomas MD PhD⁴, Francesco Ciccia MD PhD²

¹Dipartimento PROMISE, Section of Rheumatology, University of Palermo, Palermo, Italy

²Dipartimento di Medicina di Precisione Università degli Studi della Campania “Luigi Vanvitelli, Naples, Italy

³UOC di Anatomia Patologica, Azienda Ospedaliera Ospedali Riuniti Villa Sofia-Cervello, Palermo, Italy

⁴Dipartimento di Biopatologia e Biotecnologie Mediche, Università di Palermo, Italy

⁵The University of Queensland Diamantina Institute, Princess Alexandra Hospital, Brisbane, QLD, Australia

⁶ National Institute for Health Research (NIHR) Guy’s and St Thomas’ Biomedical Research Centre (BRC), London, United Kingdom.

⁷Institute of Infection, Immunity and Inflammation, University of Glasgow, Glasgow, UK

⁸Skeletal Biology and Engineering Research Center, University of Leuven

⁹Molecular Immunology and Inflammation Unit, University of Ghent, Ghent, Belgium

*These authors contributed equally to this paper.

This article has been accepted for publication and undergone full peer review but has not been through the copyediting, typesetting, pagination and proofreading process, which may lead to differences between this version and the [Version of Record](#). Please cite this article as [doi: 10.1002/ART.41644](https://doi.org/10.1002/ART.41644)

This article is protected by copyright. All rights reserved

Author's disclosure: There is neither financial support nor other benefits from commercial sources to be reported for the work presented in the manuscript, nor any other financial interests that any of the authors may have, which could create a potential conflict of interest or the appearance of a conflict of interest concerning the work.

Correspondence to:

- Prof. Francesco Ciccìa, Dipartimento di Medicina di Precisione, Section of Rheumatology, Università degli Studi della Campania L. Vanvitelli, Naples, Italy; e-mail francesco.ciccìa@unicampania.it. Telephone and FAX: +39 081666654

Abstract

Background: This study evaluated the activation and functional relevance of inflammasome pathways in AS patients and rodent models and their relationship to dysbiosis.

Methods: Inflammasome pathway was evaluated in the gut and peripheral blood of 40 AS patients by RT-qPCR, IHC, flow cytometry and confocal microscopy and compared to 20 healthy controls (20) and 10 Crohn's disease patients. Silver stain visualized bacteria in human samples and antibiotics were administered to HLA-B27 transgenic rats. The NLRP3 inhibitor MCC950 was administered to SKG mice and ileal and joint tissues assessed by IHC and qRT-PCR. The role of inflammasome in modulating IL-23/IL-17 axis was studied ex-vivo.

Results: NLRP3, NLRC4 and AIM2 expression were increased in the gut of HLA-B27 TG rats and reduced by antibiotics ($p < 0.05$). In curdlan-treated SKG mice, NLRP3 blockade prevented ileitis and delayed arthritis onset ($p < 0.05$). Compared to HC, in the ileum of AS patients, NLRP3 (2.33 vs 22.2, $p < 0.001$), NLRC4 (1.90 vs 6.47, $p < 0.001$), AIM2 (2.40 vs 20.8, $p < 0.001$), Caspase-1 (2.53 vs 24.8, $p < 0.001$), IL-1 β (1.07 vs 10.93, $p < 0.001$) and IL-18 (2.56 vs 15.67, $p < 0.001$) were over-expressed and Caspase-1 activity was increased ($p < 0.01$). The score of adherent and invasive mucosa-associated bacteria was higher in AS ($p < 0.01$) and correlated with the expression of inflammasome components in PBMC ($p < 0.001$). NLRP3 expression associated with disease activity (ASDAS-CRP)

($r^2=0.28$, $p<0.01$) and *IL23A* ($r^2=0.34$, $p<0.001$). In vitro, inflammasome activation in AS monocytes was paralleled by increased serum levels of IL-1 β and IL18. The induction of *IL-23p19*, *IL-17A*, and *IL-22* was IL-1 β -dependent.

Conclusions: Inflammasome activation occurs in rodent models and AS patients, is associated with dysbiosis, and is involved in triggering ileitis in SKG mice. Inflammasome drives type 3 cytokine production with an IL-1 β -dependent mechanism in AS patients.

Funding: This work was unconditionally supported in part by a grant from MIUR, Italy.

Introduction

Ankylosing spondylitis (AS) is a chronic inflammatory disease of unknown origin, mainly affecting the axial skeleton (1). A growing body of evidence indicates that the aberrant activation of the innate immune systems drives inflammatory processes in AS (1).

IL-23 and IL-17, both regulators of both innate and adaptive immunity, have been demonstrated to be critical cytokines in AS pathogenesis (2,3), although mechanisms underlying their over-expression in AS are not entirely understood.

Recently, activation of the inflammasome has been demonstrated to induce the release of IL-23 and IL-17 in human mononuclear cells (4). The inflammasomes are innate immune system receptors and sensors that control the inflammatory response and coordinate antimicrobial host defenses (5). Inflammasome is activated by pathogen-associated molecular (PAMPs) and danger-associated molecular patterns (DAMPs) following the detection of pathogenic microorganisms and danger signals in host cells' cytosol. Once activated, inflammasomes trigger inflammatory caspase-1, thus inducing pro-inflammatory cytokines such as IL-1 β and IL-18 and pyroptotic cell death.

Dysregulated inflammasome activity has been implicated in hereditary and acquired inflammatory disorders (6). Variations in genes encoding proteins directly or indirectly involved in regulating inflammasome activity are associated with AS, including *MEFV*, *CARD9*, *CARD15*, *IRGM*, *IL1R1* and *IL1R2* [reviewed in (7)]. Studies on the role of the inflammasome in the pathogenesis of AS have been mainly limited to peripheral blood monocytes (8).

In this study, we aimed to investigate the expression of inflammasome components in inflamed tissues of AS patients and two well-documented rodent models of spondyloarthritis – HLA-B27 rats and curdlan-treated SKG mice [reviewed in (9)]; finally, we looked at the effect of intestinal bacteria in modulating inflammasome and the inflammasome role in modulating type III cytokine.

Methods

Patients

Thirty-five HLA-B27 AS patients fulfilling the New York AS diagnostic criteria (10) and with active disease defined as an AS Disease Activity Score (ASDAS) (11) ≥ 2 were enrolled at the University of Palermo (IT). Baseline characteristics of patients and

controls are shown in Supplementary Table 1. All the patients underwent ileocolonoscopy and multiple adjacent ileal mucosal biopsies independently of the presence of gastrointestinal symptoms. Additional ten patients affected by Crohn's disease (CD) with active disease were considered as positive controls. Thirty gender and age-matched healthy controls undergoing ileocolonoscopy for diagnostic purposes without evidence of intestinal disease were considered as controls. Paired formalin-fixed paraffin-embedded (FFPE) tissue and tissue RNA were prepared from all patients to allow cross-referencing between histological assessments and qPCR gene expression analysis. As previously described ileal samples obtained from patients with AS were histologically classified into three phenotypes, normal gut histology, acute and chronic inflammation (12). Histological scoring is further detailed in Supplementary Methods.

Immunohistochemistry

After heat-induced antigen retrieval, immunohistochemistry (IHC) for AIM2, NLRP3, NLRC4, IL1 β and IL-18 was performed on 5- μ m-thick paraffin-embedded sections from ileal samples as previously described (13). Primary and secondary antibodies are shown in Supplementary Table 2.

Confocal microscopy analysis for GSDMD-NT

The accumulation of the N-terminal cleavage product of gasdermin D (GSDMD-NT) was used as a read-out for the occurrence of pyroptosis in tissue, as previously described (14). Double immunostaining was performed using an antibody against the N-terminal cleavage product of Gasdermin-D (GSDMD-NT) and DAPI, and the images were evaluated by confocal microscopy. The membrane localization of GSDMD-NT was assessed by counting the positively stained cells on photomicrographs obtained from 3 random high-power microscopic fields (400X magnification).

Transcriptomic analysis

Sixty-six AS cases (defined by the modified New York Criteria) and 78 healthy controls with no diagnosed inflammatory disease were recruited for the transcriptomic analysis (see supplementary table 3). Human ethics approval was granted by the Princess Alexandra Hospital and The University of Queensland Ethics Committees (ethic no. Metro South HREC/05/QPAH/221 and UQ 2006000102), and written informed consent was received from all participants before inclusion in the study. RNA was extracted from peripheral blood mononuclear cells, reverse transcribed, prepared for sequencing using

Illumina TruSeq Standard Total RNA Library Prep Kit. Total RNA-sequencing was performed using an Illumina HiSeq 2000 with a mean of 56M reads per sample. Transcripts were quantified using Salmon (version 0.11.2) (15) using the Ensembl 94 transcript model. Gene level differential expression analysis was performed using DESeq2 (version 1.22.1) (20), correcting for patient sex.

RNA extraction and quantitative TaqMan real-time PCR (RT-PCR)

Gut samples were stored in RNA-later at -80° until extraction. Total RNA was extracted using the Qiagen RNeasy Mini kit, with on-column DNase I digestion as previously described (13). Gene expression was quantified by quantitative PCR using TaqMan probes and run on a 7900HT Fast Real-Time PCR System (Life Technologies). Gene expression was normalized against housekeeping genes, namely *18S* and *GAPDH*.

Flow cytometry analysis of surface and intracellular antigens

Peripheral Blood Mononuclear Cells (PBMCs) were isolated from ten AS patients and ten healthy controls by Ficoll-Paque density gradient centrifugation, as previously described (13). PBMCs were stored in liquid nitrogen, then thawed, immunostained, and analyzed on a BD LSR Fortessa cytometer. The antibody panel is provided in Supplementary Methods.

ELISA for circulating IL-1 β , LPS and IL-18

IL-1 β , LPS and IL-18 were quantified by ELISA (Thermofisher) in serum isolated immediately after collection, flash-frozen, and stored at -80°C until analysis. All results were analyzed using a five parameter-logistic (5PL) function for fitting standard curves obtained from recombinant protein standards.

Isolation and culture of bacteria

Bioptic specimens of the ileum were analyzed for the bacteriological study. According to Conte et al., the samples were immediately processed to isolate and culture adherent bacteria (17); for further details, see Supplementary Methods.

Cell cultures

Isolated monocytes from 7 AS patients and 7 controls were incubated with LPS (0.1 $\mu\text{g/ml}$). The expression of inflammasome components and the cytokines IL-23, IL-18, and IL-1 β were quantified by RT-PCR, and the levels of IL-1 β and IL-18 in the supernatants measured by ELISA (Thermofisher).

Fluorometric detection of active cellular Caspase 1

A fluorescence-labeled inhibitor specific for Caspase-1 (FLICA) (Sigma Aldrich) was used according to the manufacturer's instructions to determine the Caspase-1 activity in isolated lamina propria mononuclear cells (LPMC), PBMC, and peripheral monocytes. LPMCs were obtained as described by van Damme N et al. (18). Further details are provided in Supplementary Methods.

HLA-B27 TG rats

HLA-B*2705 transgenic rats of line 33-3 (B27-TG) on a Fischer background (F344/NTac-Tg (HLA-B*2705, β 2M) (Taconic, Hudson, NY) were backcrossed with PVG rats (PVG/OlaHsd) (Harlan, UK) for a minimum of ten generations before their use in experiments. Wild type PVG rats (PVG/OlaHsd) were purchased from Harlan and bred in-house. Animals were screened for expression of HLA-B27 by flow cytometry. Age-matched non-transgenic littermates were used as controls.

All procedures were approved by the University of Glasgow Ethical Review Panel and performed under licenses from the UK Home Office under the Animal [Scientific Procedures Act 1986]. Details on animal treatments are reported in Supplementary Methods.

SKG mice

Female BALB/c and SKG mice (ZAP-70^{w163c}-mutant BALB/c mice) (n=5/group), originally obtained from S. Sakaguchi (University of Kyoto) were bred and housed under SPF or germ-free conditions at The University of Queensland Translational Research Institute (TRI) Animal Facility under the guidelines of University of Queensland (UQBR). Mice were under a 12-hours light/dark cycle, with food and water provided ad libitum. Mice were used 8-12 weeks of age. Approval for all experiments was obtained from The University of Queensland animal ethics committee.

Where indicated, female SKG mice (n=5 per group based on effect size and variance from previous experiments) were randomized to receive inflammasome inhibitor MCC950 (0.3 mg/kg, a gift of A/Prof Avril Robertson, UQ IMB) or vehicle in the drinking water starting one day before or seven days after i.p. administration of 15mg/ml 1,3- β -glucan (curdlan) in saline. For further details see Supplementary methods.

Isolation of murine intestinal cells, RNA extraction and qPCR

The intraepithelial lymphocytes (IEL) were isolated from naïve and 7 days curdlan-treated BALB/c and SKG small intestine (SI) after dissecting Peyer's patches and fat removal.

For further details see Supplementary Methods. Briefly, small intestines were collected and cut open longitudinally after removing Peyer's patches (PP), washed in cold PBS, dissected into 1-2 cm pieces and then shaken in HBSS containing 5 mM EDTA for 20 minutes at 37°C. Intraepithelial mononuclear cells were collected after passing through a 70 µm strainer. IEL cells were then harvested from the interphase of a 40% Percoll gradient after centrifugation at 20°C. Total RNA was isolated using RNeasy mini kit (Qiagen) and cDNA was prepared using Tetro cDNA synthesis kit (Bioline). Quantitative real-time PCR for *Nlrp3*, *Nlrc4*, *Nlrp6*, *Aim2*, *Nlrp12*, *Il18* and *hprt* was performed using SYBR green technique (Primer sequences shown in Supplementary Methods). All data are reported as relative fold change compared to *hprt*.

Study approval

The study was conducted according to the Declaration of Helsinki. Consent was obtained from all enrolled subjects after the nature of the investigation was explained and in accordance with the approved protocol from the institutional review board at the Universities of Palermo, Gent, and Brisbane. The appropriate institutional review boards at the University of Glasgow and Brisbane approved animal studies.

Statistical analysis

The non-parametric Mann–Whitney test was used to calculate the statistical significance between groups. Spearman's rank correlation was used to calculate the correlation between different variables in AS. p values <0.05 were considered significant.

Results

Inflammasome is activated in the gut of HLA-B27 rats and SKG mice

We first examined the expression of inflammasome related genes in the gut of two models of AS. In the gut of HLA-B27 TG rats, NLRP3, NLRC4 and AIM2 expression was increased and significantly reduced after antibiotics treatments (Figure 1), indicating that dysbiosis upregulates the expression of inflammasome components, namely NLRP3, NLRC4 and AIM2 in the ileum.

In the SKG model, among the inflammasome components tested (Supplementary Figure 1) the upregulation of *NLRP3* and *IL18* mRNA (Figure 2A-B) was observed in the intraepithelial cells of curdlan-treated SKG but not BALB/c mice. Interestingly, blocking NLRP3 activation with the MCC950 inhibitor just before curdlan in SKG mice suppressed gut disease and prevented weight loss (Figure 2C), but not after (data not shown).

Conversely, in the same of curdlan-treated SKG mice the prophylactic blockade of NLRP3 by MCC950 delayed the onset of the articular manifestations, but the difference in arthritic score was lost by day 26 (Figure 2D). Interestingly, mesenteric lymph node NKp46⁺ ILC expanded in mice treated with MCC950 while NKp46⁻ ILC decreased, without any changes in monocytes or T cells (Figure 2F).

Inflammasome in AS gut

Next, inflammasome activation was assessed in AS gut. A significant increase in expression levels of *NLRP3* (Figure 3 A-B), *NLRC4* (Figure 3C-D) and *AIM2* (Figure 3E-F) at both mRNA and protein levels was observed in the inflamed gut of AS patients, especially in those with chronic gut inflammation compared to HCs and CD patients. *NLRP3*, *NLRC4* and *AIM2* protein expression was mainly observed among inflammatory infiltrating mononuclear cells and epithelial cells. Increased expression of other inflammasome-related genes such as *NLRP6* (Supplemental Figure 2A), *NLRP12* (Supplemental Figure 2B) and *NLRC3* (Supplementary Figure 2C) was also observed in AS ileal samples. Over-expression of inflammasome components in AS gut was associated with the significantly increased expression of *Casp1* mRNA (Figure 4 A). Consistently, the use of a fluorochrome-labeled inhibitor peptide that binds specifically the active site of the Caspase-1 demonstrated the increased activation of Caspase-1, and in turn inflammasome, in the frozen section of AS gut and isolated LPMC (Figure 4 B-C).

Similarly, in AS associated chronic gut inflammation IL-1 β and IL-18 expression was increased at both mRNA and protein level (Figure 4 D-E).

Inflammasome-related pyroptosis in AS gut

Activation of caspase 1 induces human gasdermin D's cleavage to generate an N-terminal cleavage product (GSDMD-NT) that causes pyroptosis by forming membrane pores and stimulate the release of inflammatory cytokines (14). The cellular distribution of GSDMD-NT was assessed by confocal microscopy in paraffin-embedded ileal sections, using an anti-GSDMD-NT monoclonal antibody: a predominant GSDMD-NT membrane localization in AS patients compared to controls where it was mainly cytosolic (Figure 4 F).

Dysbiosis drives inflammasome activation in AS

As previously demonstrated (19), AS ileal biopsies featured the presence of adherent and invading bacteria that were scored (data not shown). A significant positive correlation was observed between the intestinal bacterial score and the expression levels of *NLRP3*, *NLRC4* and *AIM2* (Supplementary Figure 3A-C). The concentration of mucosa-associated bacteria after the fourth wash and hypotonic lysis from the ileum, caecum, and rectum biopsy specimens of patients with AS and CD was compared with controls. In the ileum, total aerobe and facultative-anaerobe counts and total Gram-negative bacterial counts were significantly higher in patients with AS, especially in those with chronic gut inflammation (Supplemental Table 3). Only isolated bacteria from the gut of AS patients, but not from controls, significantly increased the expression of *NLRP3* (Supplemental Figure 3D) and *AIM2* (Supplemental Figure 3E), but not of *NLRC4* (Supplemental Figure 3F) in PBMC isolated from HCs.

Inflammasome components are over-expressed in AS PBMC and associated with increased IL-1 β and IL-18 serum levels

We have previously demonstrated an increased concentration of gut-derived bacterial products and immune cells in the systemic circulation of AS patients as a consequence of the leaky gut (19,20). In this study, we confirm the increased concentration of LPS in the serum of AS patients previously described (Figure 5A). We hypothesized that increased LPS concentration could be responsible for an inflammasome up-regulation in AS PBMC. For this purpose, we performed the analysis of gene expression by RNA-Seq of PBMC obtained from 66 AS patients demonstrating the over-expression of inflammasome related genes as highlighted by the significantly increased expression of *NLRP3* ($p=6 \times 10^{-8}$), *Caspase-1* ($p=0.006$), *IL1 β* ($p=5 \times 10^{-12}$) and *IL18* ($p=0.00017$) and the increased expression of *NLRC4* although not statistically significant ($p=0.06$) (data not shown). RT-PCR next confirmed inflammasome over-expression in isolated circulating monocytes obtained from further 30 AS patients. In isolated unstimulated monocyte, the expression levels of *NLRP3*, *NLRC4* and *AIM2* was higher in AS compared with controls (Figure 5B). The increased expression of *NLRP3*, *NLRC4* and *AIM2* was accompanied by the over-expression of *caspase-1*, *IL-1 β* , *IL-18* and *IL-23p19* (Figure 2 B). The staining with FLICA, binding the active caspase-1, also confirmed the exaggerated inflammasome activation in AS monocytes (Figure 5C). Activation of the inflammasome in AS monocytes was independent of medications (data not shown). Analysis of IL-1 β and IL-18 serum

concentrations in AS patients demonstrated that IL-1 β serum levels and IL-18 (Figure 5D) were higher in patients with AS than in normal controls.

Interestingly, a significant correlation was found between *NLRP3* (Figure 5 E), *AIM2* ($r^2=0.3466$, $p=0.0018$, data not shown) and *NLRC4* ($r^2=0.4432$, $p=0.0011$, data not shown) expression and the disease activity as assessed by ASDAS-CRP and between *NLRP3* and *IL23A* (Figure 5 F).

We next studied the in vitro effect of LPS on monocytes isolated from AS and controls. In vitro, the stimulation of isolated AS monocytes with LPS induced a significant up-regulation of *NLRP3*, *NLRC4*, and *AIM2*, as expected. However, AS monocyte showed hyper-responsiveness to LPS compared to HC (Figure 6 A-C).

Inflammasome modulates IL-23, IL-17 and IL-22 expression through IL-1 β induction

Inflammasome has been recently demonstrated to modulate the release of IL-23 and IL-17 in human monocytes (4). In consideration of the key role of IL-23 and IL-17 in the pathogenesis of AS (1,3), we next evaluated the role of inflammasome in modulating IL-23 and IL-17 production. The administration of LPS (Figure 6 D) significantly increased IL-23 expression. To test whether the LPS induced IL-23 expression was partially mediated by inflammasome activation, KCl, known to block inflammasome activation, was administered. The addition of KCl was able to suppress IL-23 expression, inhibition reverted by the co-incubation with IL-1 β (Figure 6 D). Similarly, the inflammasome inhibition significantly reduced the expression of IL-17 and IL-22 in isolated PBMC that was rescued by IL-1 β addition (Figure 6 E-F).

Discussion

AS is a chronic inflammatory condition characterized by the genetic association with the MHC class I molecule, HLA-B27 (1). This association has previously suggested a predominant adaptive immune activation in the pathogenesis of AS. Although a direct role of IL-1 β and IL-18 in the pathogenesis of AS is still not clear, both *ILR1* and *IL1R2* are definitively associated with AS (21).

Clinical studies on the IL-1 receptor antagonist anakinra in AS patients demonstrated contrasting results, suggesting that this agent may not be highly effective in AS (22,23). The present study shows that: (1) inflammasome signaling is up-regulated and activated in the inflamed gut of AS patients; (2) dysbiosis drives inflammasome activation in AS; (3) inflammasome activation occurs in AS monocytes and is associated with increased serum levels of IL-1 β ; (4) inflammasome modulates IL-23, IL-17 and IL-22 expression through IL-1 β induction.

The inflammasome is a cellular multiprotein complex mainly associated with innate immune system signaling that through the activation of caspase-1 induces the maturation of IL-1 β and IL-18 in the active forms (5). NLRs and AIM2, the most important inflammasome cytosolic sensors responding to a great variety of endogenous and exogenous ligands (5), were over-expressed in the inflamed gut of HLA-B27 transgenic rats and small intestinal lymphocytes after curdlan-treatment of SKG mice and in AS and CD patients.

Interestingly, the level of expression of the inflammasomes components was higher in the intestine of patients with AS, especially in those with chronic gut inflammation where higher bacterial loads was observed, than in CD. This observation may support the hypothesis of a disease-specific (possibly bacterial-dependent) activation of the inflammasome in AS, rather than an unspecific effect linked to the presence of an intestinal inflammation. AS patients and CD patients have been demonstrated to have a different microbiome composition and this might be, at least in part, responsible for the different degrees of inflammasome activation. We cannot exclude that disease-related factors might also be responsible for the differences observed. Beyond the over-expression of the inflammasome components, inflammasome activation is known to trigger cleavage, activation and secretion of pro-inflammatory IL-1 β and IL-18, which in

turn activate multiple cells aiming to increase the antimicrobial program and initiate the Th1 and Th17 responses (24).

The functional relevance of inflammasome over-expression in the AS gut is supported by the demonstration of the activation of caspase-1 in the inflamed gut of AS associated with the increased expression IL-1 β and IL-18. Activation of caspase 1 also induces human gasdermin D cleavage to generate a pore-forming N-terminal cleavage product (GSDMD-NT) that triggers pyroptosis, a highly inflammatory form of programmed cell death. Pyroptosis amplifies the inflammatory process, initiating the secretion of inflammatory cytokines and releasing the intracellular content providing a high load of damage-associated molecular patterns (DAMPs) (25). Tissue analysis of GSDMD-NT, assessed by confocal microscopy in paraffin-embedded ileal sections, showed a significant shift GSDMD-NT from a cytosolic to a membrane localization, confirming the occurrence of pyroptosis in AS patients (14).

The results of the present study do not clarify the causes of activation of the inflammasome pathway. It cannot be ruled out that, in an auto-inflammatory fashion, genetic factors predisposing to the disease may be per se associated with a greater expression and activation of this pathway. On the other hand, it is plausible that genetic predisposition may significantly influence the host's immune responses to environmental factors, particularly the capacity of pathogenic and non-pathogenic microorganisms to trigger inflammasome activation after breaching the epithelial barrier.

In this regard, intestinal dysbiosis observed in AS, and rodent models (26) is relevant to innate immune responses' modulation. Although a direct pharmacological action on innate intestinal immune mechanisms cannot be excluded, the effect of the antibiotics on the expression of the inflammasome components in the gut of HLA-B27 TG rats may suggest that an altered composition of the intestinal flora can be responsible for the innate immune activation present in the intestine of patients with AS.

Consistently, isolated ileal bacteria from AS ileum significantly increased the expression levels of *NLRP3* and *AIM2* in isolated PBMC. Interestingly, no significant modulation of *NLRC4* was observed in in vitro studies. The *NLRC4* inflammasome relies on NLR family apoptosis inhibitory proteins (*NAIPs*) for sensing bacterial components in the cytosol (27). The difficulty in activating *NLRC4* in vitro studies has been demonstrated in other works such as that of Karki et al. (28), in which there was no significant induction of *Nalps*

in vitro in response to infection. The demonstration of the strong positive correlation between the bacterial scores and the expression levels of *NLRP3*, *NLRC4* and *AIM2* further supports this hypothesis together with inflammasome expression induced by isolated bacteria from the gut of AS.

While in human AS or B27 rats, it is not clear whether the activation of the inflammasome is a consequence or a cause of the intestinal inflammation, we demonstrate that the NLRP3 inflammasome inhibitor MCC950 suppresses the onset of intestinal inflammation in SKG mice when introduced before but not after the Curdlan administration. These data strongly suggest that curdlan stimulates NLRP3 inflammasome activation by enhancing host-bacterial interaction (29), which is required to trigger intestinal inflammation (30). The delayed arthritis onset further suggests its initial dependence on inflammasome activation. Once triggered, intestinal inflammation is no longer susceptible to inflammasome inhibition due to reliance on other mediators, such as IL-17 (31). Interestingly, MCC950 expanded NCR⁺ but not NCR⁻ ILC3 cells. In this regard, NCR⁺ ILC3s have been demonstrated to be important in controlling mouse colonic infection with *Citrobacter rodentium* in the presence of T cells and are essential for cecal homeostasis in mice (32).

Their expansion by MCC950 may contribute to intestinal protection due to improved bacterial control in curdlan-treated SKG mice. Studies of dysbiosis in MCC950-treated naïve SKG mice would be of interest.

As a consequence of gut inflammation, alteration of gut-epithelial and gut-vascular barriers occurs in AS and contributes to the translocation of bacterial products such as LPS, iFABP and LPS-BP into the bloodstream (19). The increased level of LPS in AS serum seems to be relevant in modulating the systemic innate immune response. In AS, the chronic circulating monocyte exposure to serum LPS induced an anergic phenotype by downregulating the expression of CD14 and reduced the expression of HLA-antigen D Related (HLA-DR) (19). LPS has been demonstrated to prime the inflammasome pathway (33) and in line with this evidence, LPS could be one of the key determinants of inflammasome upregulation in AS monocytes. Accordingly, inflammasome priming was observed in circulating unstimulated PBMC from AS patients by RNAseq and confirmed in isolated AS monocytes, where a significant correlation between *NLRP3* expression and disease activity as assessed by ASDAS-CRP was found. The functional relevance of

the increased expression of the inflammasome in AS monocytes was further supported by demonstrating Caspase 1 activation in circulating monocyte of AS and increased serum levels of IL-1 β and IL-18.

Innate immune activation has been demonstrated to predominate in AS patients with IL-23-dependent production of IL-22 and IL-17 by innate immune cells (13,34,35). Here we demonstrated that inflammasome activation might be responsible for the production of IL-23 in AS monocytes and IL-17 and IL-22 in PBMC in an IL-1 β dependent IL-23-independent way. The possibility that innate immune mechanisms independent of IL-23 operate in modulating type 3 immunity in AS, could suggest a relatively important role of IL-23 in maintaining the inflammatory process in AS, as also indicated by murine studies in which IL-23 is fundamental for the initiation but not for the maintenance of the disease (36). In *in-vitro* experiments, we demonstrated that blocking inflammasome by incubating PBMC with KCl, a known to inhibits inflammasome activation (37), significantly reduced the expression of IL-23 induced by LPS and of IL-17 and IL-22 induced by PMA and ionomycin. This effect seems to be specifically mediated by IL-1 β since the addition of recombinant IL-1 β to isolated monocytes was able to restore the production despite the inflammasome blockade.

In conclusion, in this study, we provide the first demonstration that inflammasome activation occurs in the gut of AS patients, potentially being a critical inflammatory pathway involved in the pathogenesis of gut inflammation and pro-inflammatory type 3 cytokines production.

References

1. Taurog JD, Chhabra A, Colbert RA. Ankylosing Spondylitis and Axial Spondyloarthritis. *N. Engl. J. Med.* [Internet]. 2016;374:2563–2574. Available from: <http://www.nejm.org/doi/10.1056/NEJMra1406182>
2. Ciccia F, Bombardieri M, Principato A, Giardina A, Tripodo C, Porcasi R, et al. Overexpression of interleukin-23, but not interleukin-17, as an immunologic signature of subclinical intestinal inflammation in ankylosing spondylitis. *Arthritis Rheum.* [Internet]. 2009;60:955–965. Available from: <http://doi.wiley.com/10.1002/art.24389>
3. Sherlock JP, Joyce-Shaikh B, Turner SP, Chao C-C, Sathe M, Grein J, et al. IL-23 induces spondyloarthropathy by acting on ROR- γ ⁺ CD3⁺CD4⁺CD8⁻ enthesal resident T cells. *Nat. Med.* 2012;18:1069–1076.
4. Cowardin CA, Kuehne SA, Buonomo EL, Marie CS, Minton NP, Petri WA. Inflammasome activation contributes to interleukin-23 production in response to *Clostridium difficile*. *MBio.* 2015;
5. Lamkanfi M, Dixit VM. Mechanisms and functions of inflammasomes. *Cell.* 2014;
6. Yang C-A, Chiang B-L. Inflammasomes and human autoimmunity: A comprehensive review. *J. Autoimmun.* [Internet]. 2015 [cited 2015 May 26]; Available from: <http://www.ncbi.nlm.nih.gov/pubmed/26005048>
7. Li Z, Brown MA. Progress of genome-wide association studies of ankylosing spondylitis. *Clin. Transl. Immunol.* 2017;
8. Kim S-K, Cho YJ, Choe J-Y. NLRP3 inflammasomes and NLRP3 inflammasome-derived pro-inflammatory cytokines in peripheral blood mononuclear cells of patients with ankylosing spondylitis. *Clin. Chim. Acta.* [Internet]. 2018;486:269–274. Available from: <http://www.ncbi.nlm.nih.gov/pubmed/30138619>
9. Rahman MA, Thomas R. The SKG model of spondyloarthritis. *Best Pract. Res. Clin. Rheumatol.* [Internet]. 2017;31:895–909. Available from:

<http://www.ncbi.nlm.nih.gov/pubmed/30509448>

10. Linden S Van Der, Valkenburg HA, Cats A. Evaluation of Diagnostic Criteria for Ankylosing Spondylitis. *Arthritis Rheum.* 1984;
11. Lukas C, Landewé R, Sieper J, Dougados M, Davis J, Braun J, et al. Development of an ASAS-endorsed disease activity score (ASDAS) in patients with ankylosing spondylitis. *Ann. Rheum. Dis.* 2009;
12. De Vos M, Mielants H, Cuvelier C, Elewaut A, Veys E. Long-term evolution of gut inflammation in patients with spondyloarthritis. *Gastroenterology.* 1996;110:1696–1703.
13. Ciccia F, Guggino G, Rizzo A, Saieva L, Peralta S, Giardina A, et al. Type 3 innate lymphoid cells producing IL-17 and IL-22 are expanded in the gut, in the peripheral blood, synovial fluid and bone marrow of patients with ankylosing spondylitis. *Ann. Rheum. Dis.* [Internet]. 2015;74:1739–1747. Available from: <http://ard.bmj.com/lookup/doi/10.1136/annrheumdis-2014-206323>
14. Liu X, Zhang Z, Ruan J, Pan Y, Magupalli VG, Wu H, et al. Inflammasome-activated gasdermin D causes pyroptosis by forming membrane pores. *Nature* [Internet]. 2016;535:153–158. Available from: <http://www.nature.com/articles/nature18629>
15. Patro R, Duggal G, Love MI, Irizarry RA, Kingsford C. Salmon provides fast and bias-aware quantification of transcript expression. *Nat. Methods* [Internet]. 2017;14:417–419. Available from: <http://www.nature.com/articles/nmeth.4197>
16. Love MI, Huber W, Anders S. Moderated estimation of fold change and dispersion for RNA-seq data with DESeq2. *Genome Biol.* [Internet]. 2014;15:550. Available from: <http://genomebiology.biomedcentral.com/articles/10.1186/s13059-014-0550-8>
17. Conte MP, Schippa S, Zamboni I, Penta M, Chiarini F, Seganti L, et al. Gut-associated bacterial microbiota in paediatric patients with inflammatory bowel disease. *Gut* [Internet]. 2006;55:1760–1767. Available from:

<http://gut.bmj.com/cgi/doi/10.1136/gut.2005.078824>

18. Van Damme N, De Vos M, Baeten D, Demetter P, Mielants H, Verbruggen G, et al. Flow cytometric analysis of gut mucosal lymphocytes supports an impaired Th1 cytokine profile in spondyloarthritis. *Ann. Rheum. Dis.* 2001;
19. Ciccia F, Guggino G, Rizzo A, Alessandro R, Luchetti MM, Milling S, et al. Dysbiosis and zonulin upregulation alter gut epithelial and vascular barriers in patients with ankylosing spondylitis. *Ann. Rheum. Dis.* [Internet]. 2017;76:1123–1132. Available from: <http://ard.bmj.com/lookup/doi/10.1136/annrheumdis-2016-210000>
20. Guggino G, Rizzo A, Mauro D, Macaluso F, Ciccia F. Gut-derived CD8+ tissue-resident memory T cells are expanded in the peripheral blood and synovia of SpA patients. *Ann. Rheum. Dis.* 2019;
21. Cortes A, Hadler J, Pointon JP, Robinson PC, Karaderi T, Leo P, et al. Identification of multiple risk variants for ankylosing spondylitis through high-density genotyping of immune-related loci. *Nat. Genet.* 2013;
22. Tan AL, Marzo-Ortega H, O'Connor P, Fraser A, Emery P, McGonagle D. Efficacy of anakinra in active ankylosing spondylitis: a clinical and magnetic resonance imaging study. *Ann. Rheum. Dis.* [Internet]. 2004;63:1041–5. Available from: <http://ard.bmj.com/cgi/doi/10.1136/ard.2004.020800>
23. Haibel H, Rudwaleit M, Listing J, Sieper J. Open label trial of anakinra in active ankylosing spondylitis over 24 weeks. *Ann. Rheum. Dis.* [Internet]. 2005;64:296–8. Available from: <http://ard.bmj.com/cgi/doi/10.1136/ard.2004.023176>
24. Lasigliè D, Traggiai E, Federici S, Alessio M, Buoncompagni A, Accogli A, et al. Role of IL-1 beta in the development of human TH17 cells: Lesson from NLPR3 mutated patients. *PLoS One.* 2011;
25. Mullen LM, Chamberlain G, Sacre S. Pattern recognition receptors as potential therapeutic targets in inflammatory rheumatic disease. *Arthritis Res. Ther.*

[Internet]. 2015 [cited 2015 Jun 9];17:122. Available from:

<http://www.pubmedcentral.nih.gov/articlerender.fcgi?artid=4432834&tool=pmcentrez&rendertype=abstract>

26. Asquith MJ, Stauffer P, Davin S, Mitchell C, Lin P, Rosenbaum JT. Perturbed Mucosal Immunity and Dysbiosis Accompany Clinical Disease in a Rat Model of Spondyloarthritis. *Arthritis Rheumatol.* [Internet]. 2016;68:2151–2162. Available from: <http://doi.wiley.com/10.1002/art.39681>
27. Zhao Y, Shao F. The NAIP-NLRC4 inflammasome in innate immune detection of bacterial flagellin and type III secretion apparatus. *Immunol. Rev.* [Internet]. 2015;265:85–102. Available from: <http://doi.wiley.com/10.1111/imr.12293>
28. Karki R, Lee E, Place D, Samir P, Mavuluri J, Sharma BR, et al. IRF8 Regulates Transcription of Naips for NLRC4 Inflammasome Activation. *Cell* [Internet]. 2018;173:920-933.e13. Available from: <https://linkinghub.elsevier.com/retrieve/pii/S0092867418302320>
29. Ruutu M, Thomas G, Steck R, Degli-Esposti MA, Zinkernagel MS, Alexander K, et al. β -glucan triggers spondylarthritis and Crohn's disease-like ileitis in SKG mice. *Arthritis Rheum.* [Internet]. 2012;64:2211–22. Available from: <http://www.ncbi.nlm.nih.gov/pubmed/22328069>
30. Rehaume LM, Mondot S, Aguirre de Cárcer D, Velasco J, Benham H, Hasnain SZ, et al. ZAP-70 genotype disrupts the relationship between microbiota and host, leading to spondyloarthritis and ileitis in SKG mice. *Arthritis Rheumatol.* (Hoboken, N.J.) [Internet]. 2014;66:2780–92. Available from: <http://www.ncbi.nlm.nih.gov/pubmed/25048686>
31. Benham H, Rehaume LM, Hasnain SZ, Velasco J, Baillet AC, Ruutu M, et al. Interleukin-23 mediates the intestinal response to microbial β -1,3-glucan and the development of spondyloarthritis pathology in SKG mice. *Arthritis Rheumatol.* (Hoboken, N.J.) [Internet]. 2014;66:1755–67. Available from: <http://www.ncbi.nlm.nih.gov/pubmed/24664521>

- Accepted Article
32. Rankin LC, Girard-Madoux MJH, Seillet C, Mielke LA, Kerdiles Y, Fenis A, et al. Complementarity and redundancy of IL-22-producing innate lymphoid cells. *Nat. Immunol.* [Internet]. 2016;17:179–186. Available from: <http://www.nature.com/articles/ni.3332>
 33. Ghonime MG, Shamaa OR, Das S, Eldomany RA, Fernandes-Alnemri T, Alnemri ES, et al. Inflammasome Priming by Lipopolysaccharide Is Dependent upon ERK Signaling and Proteasome Function. *J. Immunol.* [Internet]. 2014;192:3881–3888. Available from: <http://www.jimmunol.org/lookup/doi/10.4049/jimmunol.1301974>
 34. Gracey E, Qaiyum Z, Almaghlouth I, Lawson D, Karki S, Avvaru N, et al. IL-7 primes IL-17 in mucosal-associated invariant T (MAIT) cells, which contribute to the Th17-axis in ankylosing spondylitis. *Ann. Rheum. Dis.* [Internet]. 2016;75:2124–2132. Available from: <http://ard.bmj.com/lookup/doi/10.1136/annrheumdis-2015-208902>
 35. Kenna TJ, Davidson SI, Duan R, Bradbury LA, McFarlane J, Smith M, et al. Enrichment of circulating interleukin-17-secreting interleukin-23 receptor-positive γ/δ T cells in patients with active ankylosing spondylitis. *Arthritis Rheum.* [Internet]. 2012;64:1420–1429. Available from: <http://doi.wiley.com/10.1002/art.33507>
 36. van Tok MN, Na S, Lao CR, Alvi M, Pots D, van de Sande MGH, et al. The Initiation, but Not the Persistence, of Experimental Spondyloarthritis Is Dependent on Interleukin-23 Signaling. *Front. Immunol.* [Internet]. 2018;9. Available from: <https://www.frontiersin.org/article/10.3389/fimmu.2018.01550/full>
 37. Muñoz-Planillo R, Kuffa P, Martínez-Colón G, Smith BL, Rajendiran TM, Núñez G. K⁺ Efflux Is the Common Trigger of NLRP3 Inflammasome Activation by Bacterial Toxins and Particulate Matter. *Immunity.* 2013;

Legend to Figures

Figure 1. Inflammasome is upregulated in the ileum of HLA-B27 TG rats

Representative images of IHC staining performed on wild type rats (WT), HLA-B27 transgenic untreated and treated with vancomycin and meropenem for three weeks (HLA-B27+Abx) to detect NLRP3 (A), NLRC4 (B) and AIM2 (C). Quantitative analysis of NLRP3⁺ (B), NLRC4⁺ (D) AIM2⁺ (F) is shown in histograms. n=5 animal/group; **p*<0.05

Figure 2. Effect of inflammasome inhibition in SKG mice

Expression of *Nlrp3* (A), and *Il18* (B) in intestinal intraepithelial cells of BALB/c mice and SKG mice treated or not with curdlan. C: Gut inflammatory histological score and weight loss. D: mean arthritis visual score, ankle joint histological score and ear histological score of curdlan-treated SKG mice treated with the NLRP3 inhibitor MCC950 or vehicle (CTRL). E: flow cytometry quantification of mesenteric lymph node NKp46⁺ ILC, NKp46⁻ ILC, monocytes and T cells. N=5 animal/group; **p*<0.05 ***p*<0.001

Figure 3. Expression of NLRP3, NLRC4 and AIM 2 in human AS patients' ileal tissue and healthy controls (HC). A-B: mRNA levels of *NLRP3* (A), representative IHC for NLRP3 and quantification expressed as number of NLRP3⁺ cells/infiltrating cells in gut biopsies of AS and healthy control (B). C-D: : mRNA levels of *NLRC4* (C), representative IHC for NLRC4 and quantification expressed as number of NLRC4⁺ cells/infiltrating cells in gut biopsies of AS and healthy control (D). E-F: mRNA levels of *AIM2* (E), representative IHC for AIM2 and quantification expressed as number of AIM2⁺ cells/infiltrating cells in gut biopsies of AS and healthy control (F). n= 35 AS and 20 HC; **p*<0.05 versus HC.

Figure 4. Inflammasome activation in AS intestinal tissue.

A: Relative mRNA levels of *CASP1* assessed by RT-PCR in the ileal samples obtained from the AS patients and HC. B: Representative fluorescence histogram of FAM-FLICA in isolated LPMCs of HC (Red) and AS (Blue) analyzed by flow cytometry. C:

Representative confocal image of frozen AS ileum sample stained for Caspase-1 by FAM-FLICA. D: relative mRNA levels of *IL1 β* in AS and HC ileum and protein expression visualized by IHC and quantified as IL-1 β positive cells in the gut of AS patients and controls. E: relative m-RNA levels of *IL18* in AS and HC ileum and protein expression visualized by IHC and quantified as IL-18 positive cells in the gut of AS patients and controls.

F: gasdermin in the gut of AS patients observed by confocal microscopy showing a predominant membrane expression and quantification of the number of cells expressing gasdermin in the membrane and cytoplasm. n= 35 AS and 20 HC; * $p < 0.05$ ** $p < 0.01$.

Figure 5: Systemic activation of inflammasome in AS patients.

Concentration of LPS in AS and HC serum measured by ELISA is shown in (A). B: RT-qPCR data showing the expression of *NLRP3*, *NLRC4*, *AIM2*, *CASP1*, *IL1B*, *IL18*, *IL23A* plotted as fold induction on the mean of HC; n=35 AS and 20 HC. The caspase activity in circulating AS (blue) and HC (red) monocytes was assessed by FAM-FLICA staining and flow cytometry: representative fluorescence histogram and plot of mean fluorescence intensity are shown (C); n=5. D: serum levels of IL-1 β and IL-18 in AS and HC measured by ELISA. E-F: correlation between *NLRP3* expression, IL23A (E) and disease activity (ASDAS-CRP) (F). n=35 AS and 20 HC.

Figure 6: Role of inflammasome in mediating IL-23, IL-17 and IL-22 production in AS monocyte.

A-C: LPS induced expression of *NLRP3* (A), *AIM2* (B) and *NLRC4* (C) in isolated monocytes from AS patients and controls. (D) Effect of the inflammasome blocking by the addition of KCl on *IL23A* expression in human monocyte from AS patients. PMA and ionomycin induced *IL17A* (E) and *IL22* (F) expression in KCl treated AS monocyte in the presence or absence of exogenous IL-1 β . n=5, * $p < 0.05$

Supplementary Figure 1

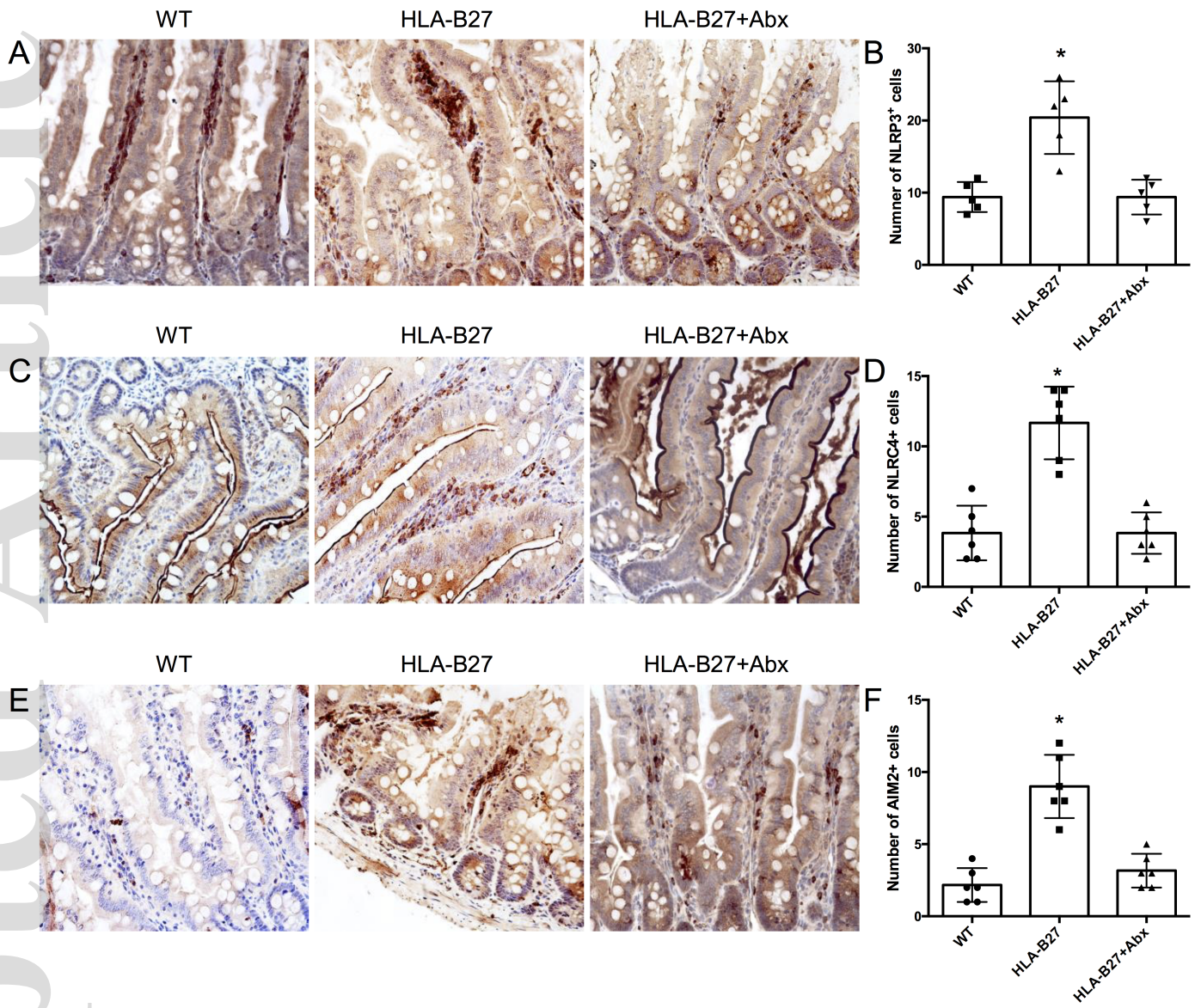
Expression of *Aim2* (A), *Nlrc4* (B), *Nlrp6* (C) and *Nlrp12* (D) in intestinal intraepithelial cells of BALB/c mice and SGK mice treated or not with curdlan. N=5 animal/group.

Supplementary Figure 2

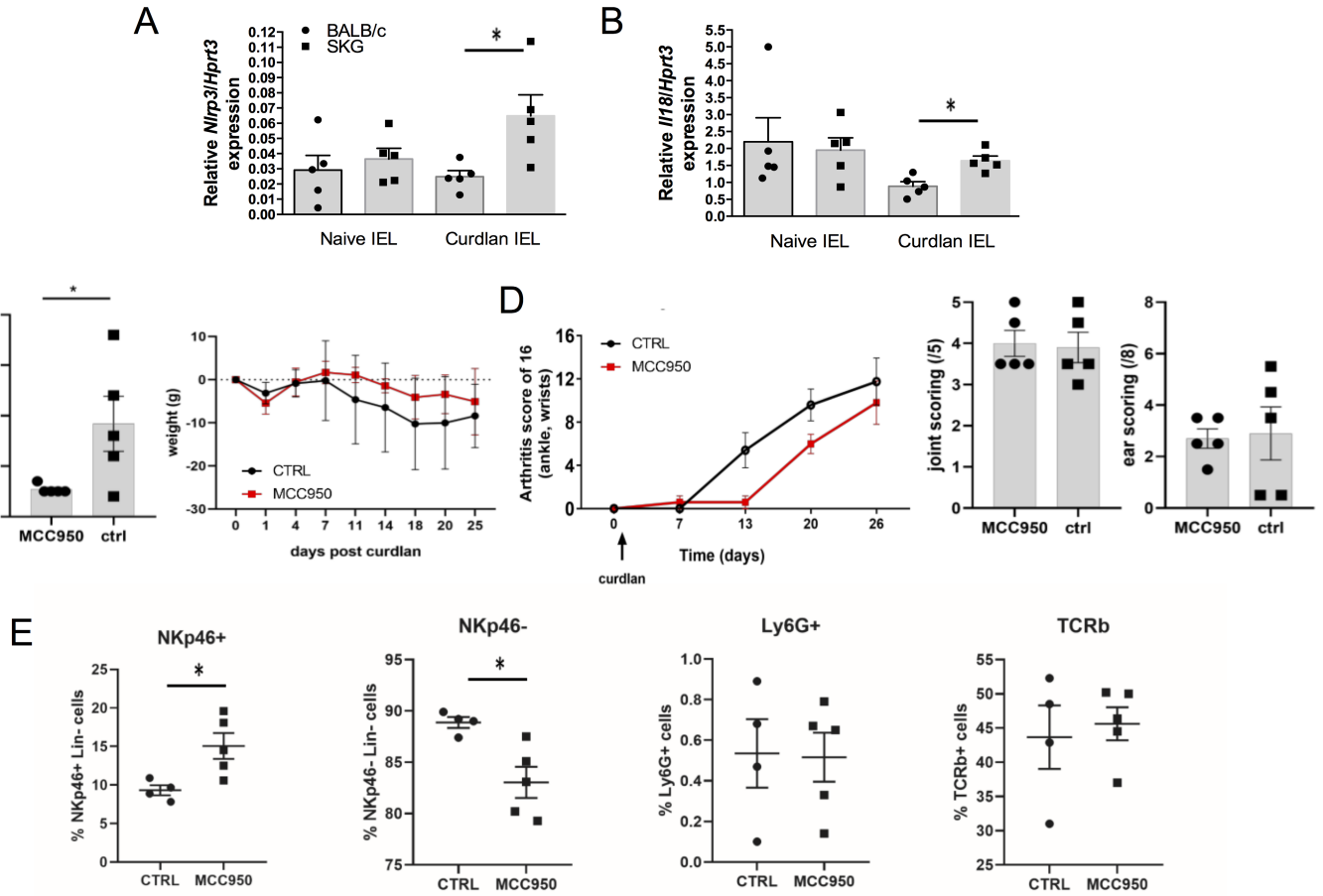
mRNA expression of *NLRC3* (A), *NLRP6* (B), and *NLRP12* (C) in ileum biopsy of AS patients and HC. n= 35 AS and 20 HC; * $p < 0.05$ versus HC.

Supplementary Figure 3

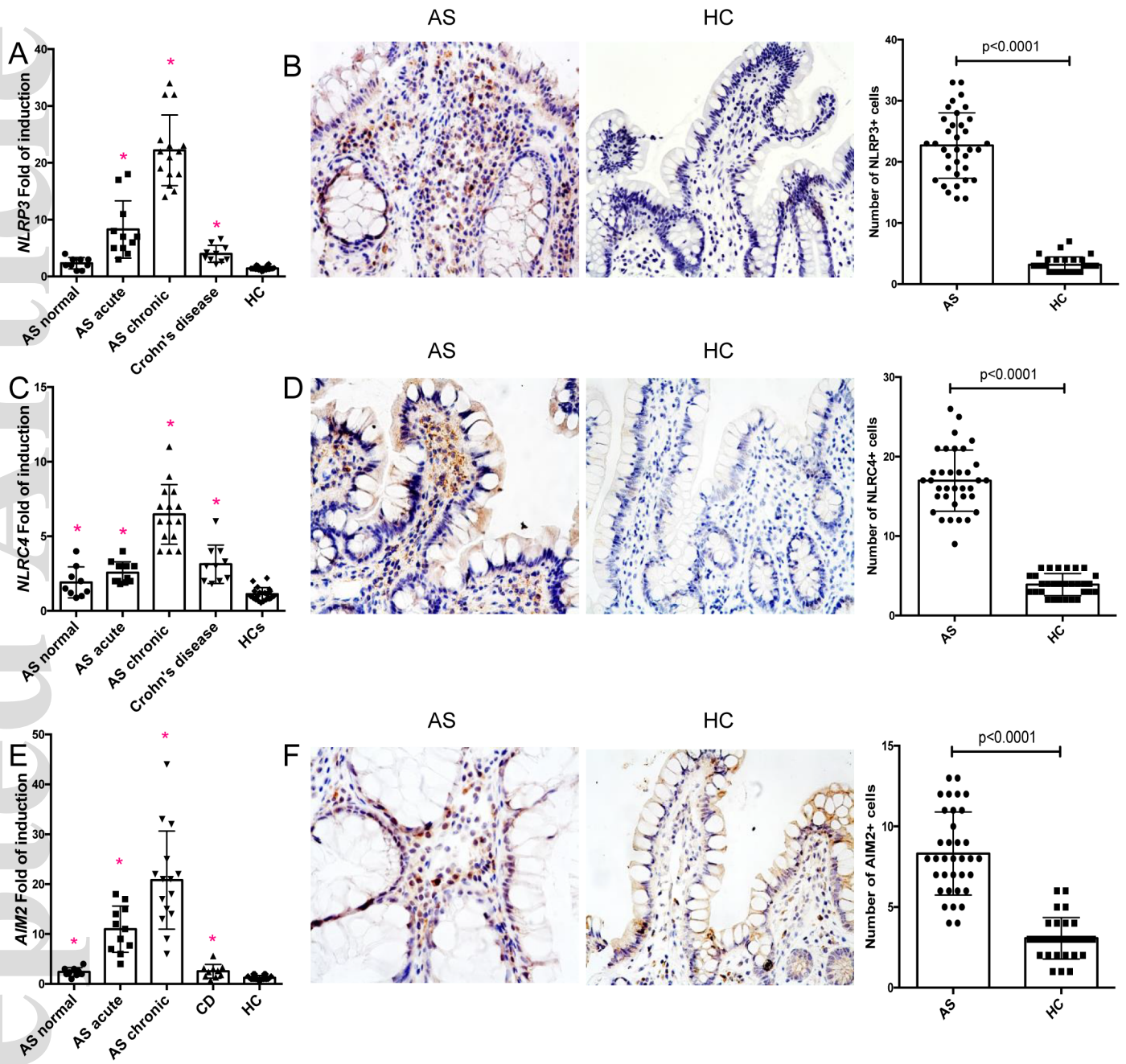
Correlation between bacterial score and mRNA expression of *NLRP3* (A), *AIM2* (B), and *NLRC4* (C) in AS ileal biopsies; n=35. In D-F mRNA expression of *NLRP3* (D), *AIM2* (E), and *NLRC4* (F) in PMBC exposed to culture media only (RPMI) or to isolated bacteria from the gut of AS patients or HC; n=5/group.



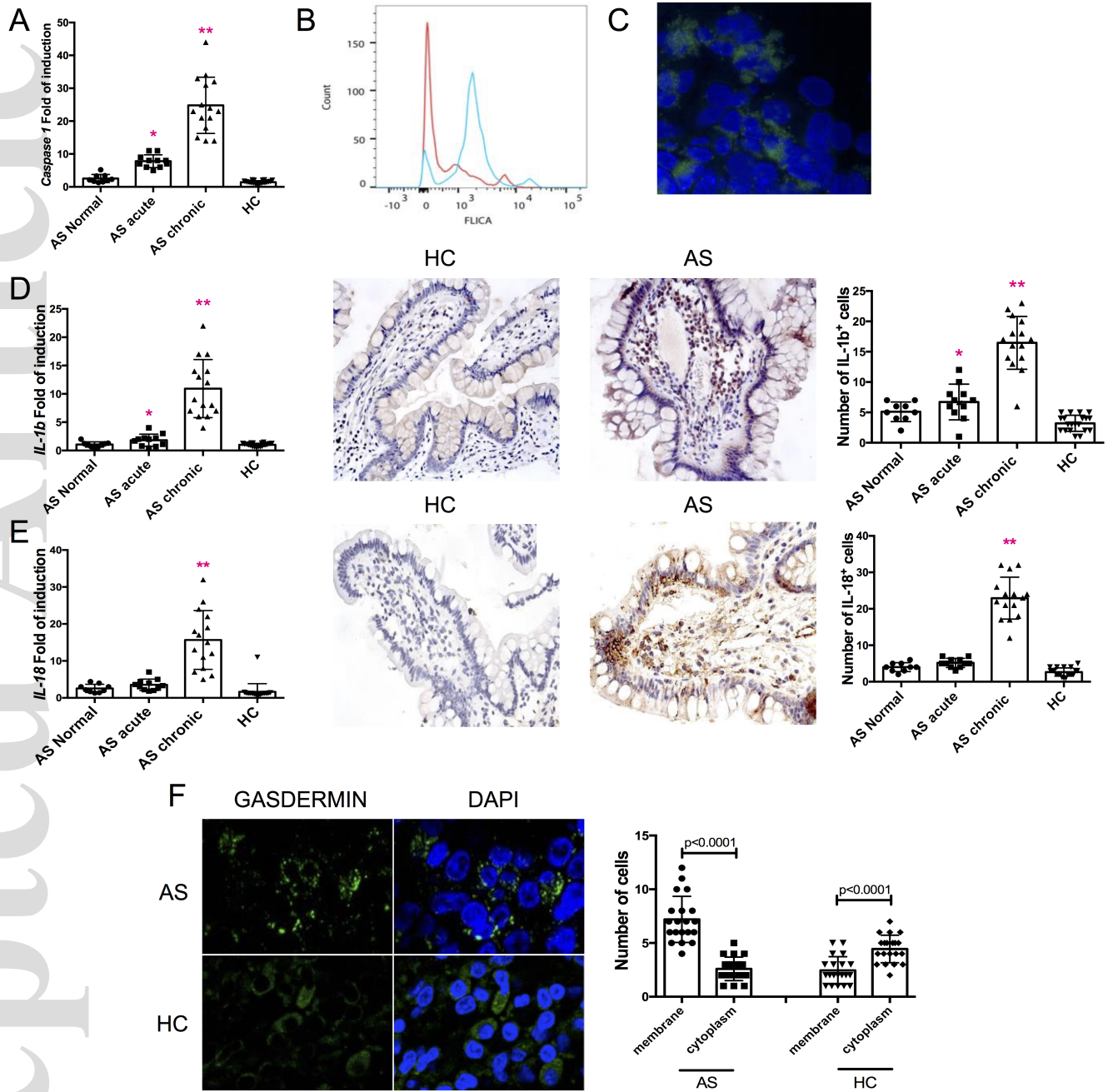
art_41644_f1.tiff



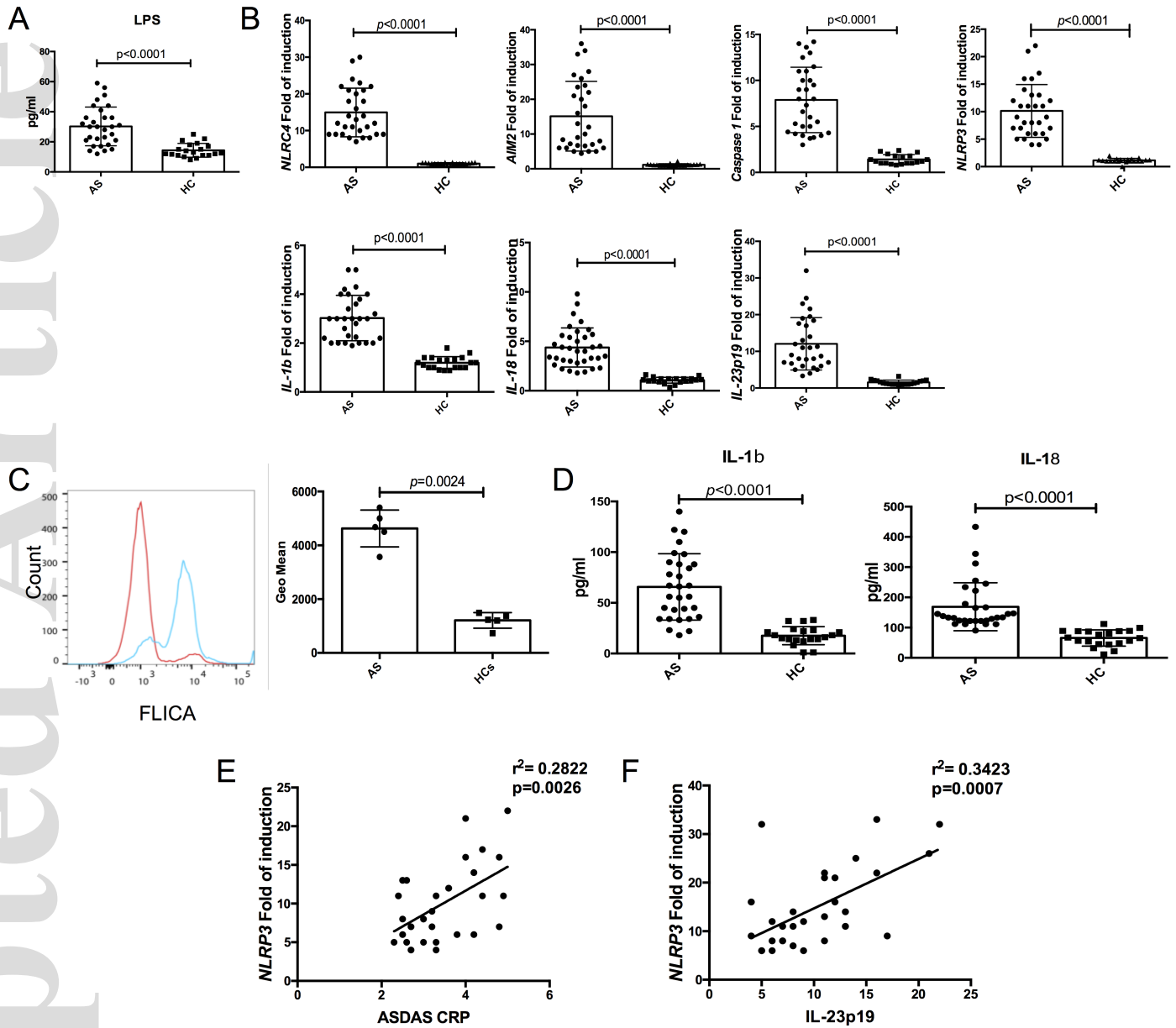
art_41644_f2.tiff



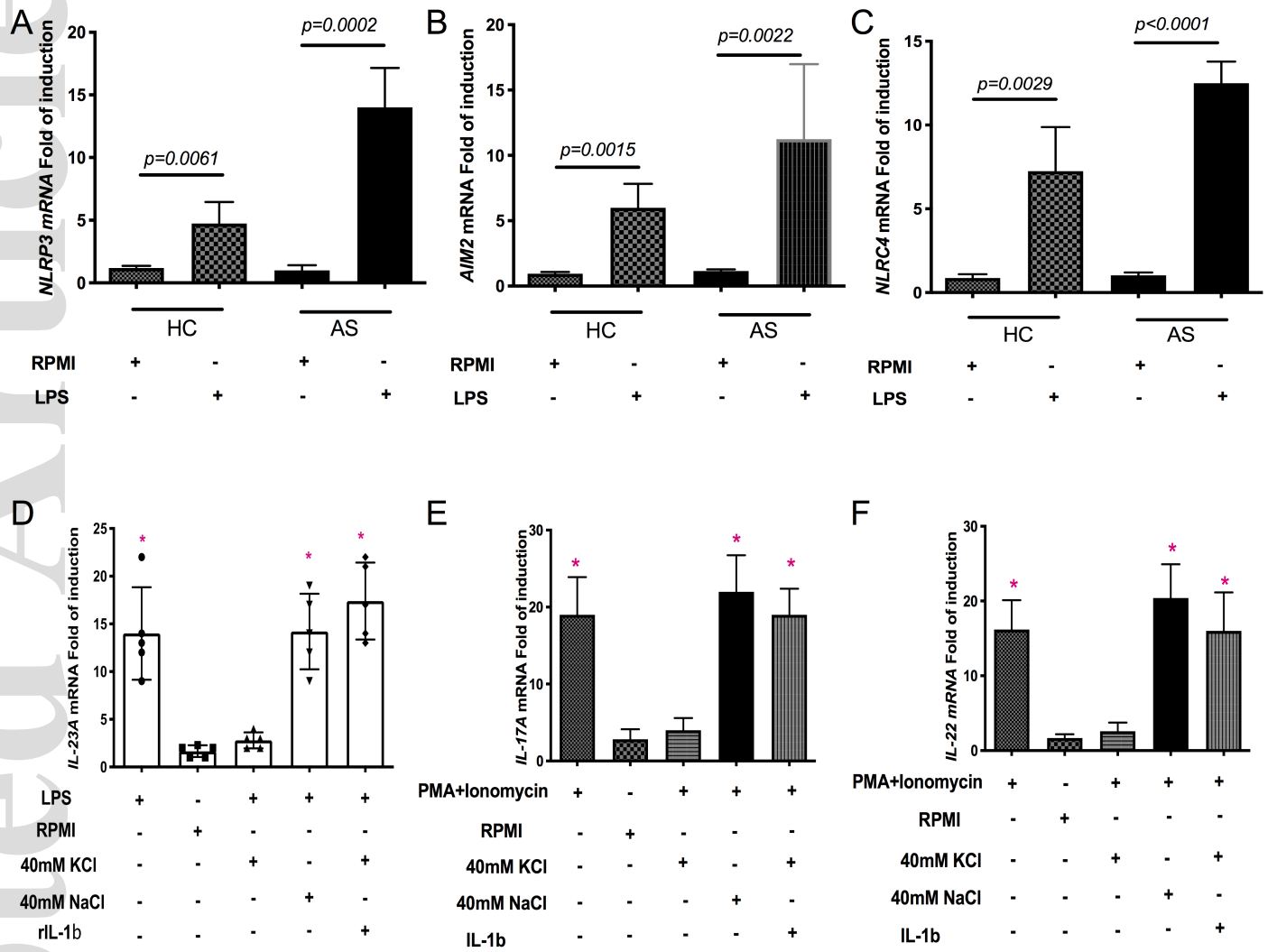
art_41644_f3.tif



art_41644_f4.tiff



art_41644_f5.tiff



art_41644_f6.tiff